# 8

Semiconductor Junctions

Almost all solar cells contain junctions between (different) materials of different doping. Since these junctions are crucial to the operation of the solar cell, we will discuss their physics in this chapter.

A *p-n* junction fabricated in the same semiconductor material, such as c-Si, is an example of an *p-n homojunction*. There are also other types of junctions: A *p-n* junction that is formed by two chemically different semiconductors is called a *p-n heterojunction*. In a *p-i-n* junctions, the region of the internal electric field is extended by inserting an intrinsic,*i*, layer between the *p*-type and the *n*-type layers. The *i*-layer behaves like a capacitor; it stretches the electric field formed by the *p-n* junction across itself. Another type of the junction is between a *metal* and a *semiconductor*; this is called a MS junction. The Schottky barrier formed at the metal-semiconductor interface is a typical example of the MS junction.

8.1 *p-n* homojunctions

8.1.1 Formation of a space-charge region in the *p-n* junction

Figure 8.1 shows schematically isolated pieces of a *p*-type and an *n*-type semiconductor and their corresponding band diagrams. In both isolated pieces the charge neutrality is maintained. In the *n*-type semiconductor the large concentration of negatively-charged free electrons is compensated by positively-charged ionised donor atoms. In the *p*-type semiconductor holes are the majority carriers and the positive charge of holes is compensated by negatively-charged ionised acceptor atoms. For the isolated *n*-type semicon-
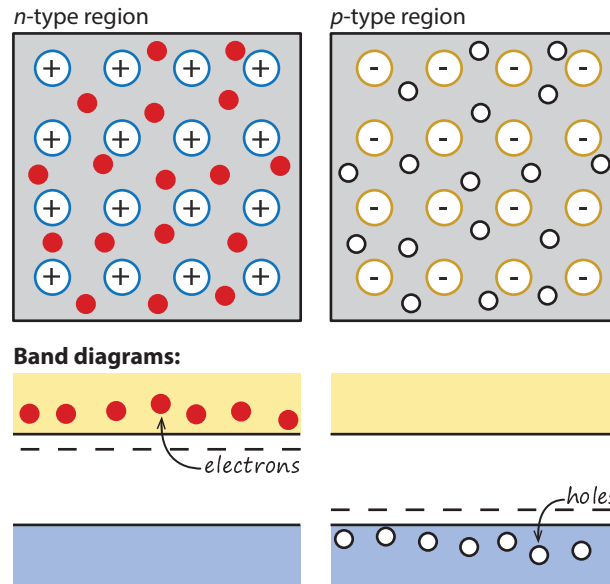
Figure 8.1: Schematic representation of an isolated *n*-type and *p*-type semiconductor and corresponding band diagrams.

ductor we can write

$$n = n_{n0} \approx N_D, \tag{8.1a}$$

$$p = p_{n0} \approx n_i^2 \big/ N_D . \tag{8.1b}$$

For the isolated *p*-type semiconductor we have

$$p = p_{p0} \approx N_A, \tag{8.2a}$$

$$n = n_{p0} \approx n_i^2 \big/ N_A . \tag{8.2b}$$

When a *p*-type and an *n*-type semiconductor are brought together, a very large difference in electron concentration between *n*- and *p*-type regions causes a diffusion current of electrons from the *n*-type material across the *metallurgical junction* into the *p*-type material. The term "metallurgical junction" denotes the interface between the *n*- and *p*-type regions. Similarly, the difference in hole concentration causes a diffusion current of holes from the *p*- to the *n*-type material. Due to this diffusion process the region close to the metallurgical junction becomes almost completely depleted of mobile charge carriers. The gradual depletion of the charge carriers gives rise to a space charge created by the charge of the ionised donor and acceptor atoms that is not compensated by the mobile charges any more. This region of the space charge is called the *space-charge* region or *depleted region* and is schematically illustrated in Fig. 8.2. Regions outside the depletion region, in which the charge neutrality is conserved, are denoted as the quasi-neutral regions.
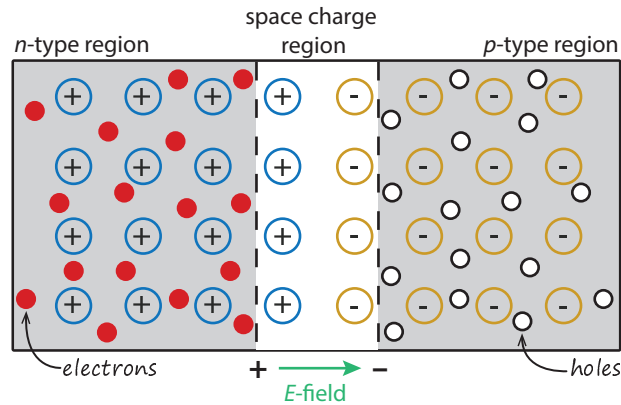
Figure 8.2:   Formation of a space-charge region, when *n*-type and *p*-type semiconductors are brought together to form a junction. The coloured part represents the space-charge region.


The space charge around the metallurgical junction results in the formation of an internal electric field which forces the charge carriers to move in the opposite direction than the concentration gradient. The diffusion currents continue to flow until the forces acting on the charge carriers, namely the concentration gradient and the internal electrical field, compensate each other. The driving force for the charge transport does not exist any more and no net current flows through the *p-n* junction.

8.1.2   The *p-n* junction under equilibrium

The *p-n* junction represents a system of charged particles in diffusive equilibrium in which the electrochemical potential is constant and independent of position. The electro-chemical potential describes an average energy of electrons and is represented by the Fermi energy. Figure 8.3 (a) shows the band diagrams of isolated *n*- and a *p*-type semiconductors. The band diagrams are drawn such that the *vacuum energy level E_{vac}* is aligned. This energy level represents the energy just outside the atom, if an electron is elevated to E_{vac} it leaves the sphere of influence of the atom. Also the electron affinity χ_e is shown, which is defined as the potential that an electron present in the conduction band requires to be elevated to an energy level just outside the atom, *i.e.* E_{vac}.

The band diagram of the *p-n* junction in equilibrium is shown in Figure 8.3 (b). Note, that in the band diagram the Fermi energy is constant across the junction, not the vacuum energy. As the Fermi energy denotes the "filling level" of electrons, this is the level that is constant throughout the junction. To visualise this, we take a look at Fig. 8.4 (a), which shows two tubes of different lengths that are partially filled with water. The filling level is equivalent to the Fermi energy in a solid state material. The vacuum energy would be the upper boundary of the tube; if the water was elevated above this level, it could leave the tube. If the two tubes are connected as illustrated in Fig. 8.4 (b), the water level in both tubes will be the same. However, the length of the tubes might be different; for leaving the first tube, a different energy can be required than for leaving the second tube.

In addition to the Fermi energy being constant across the junction, the the band-edge
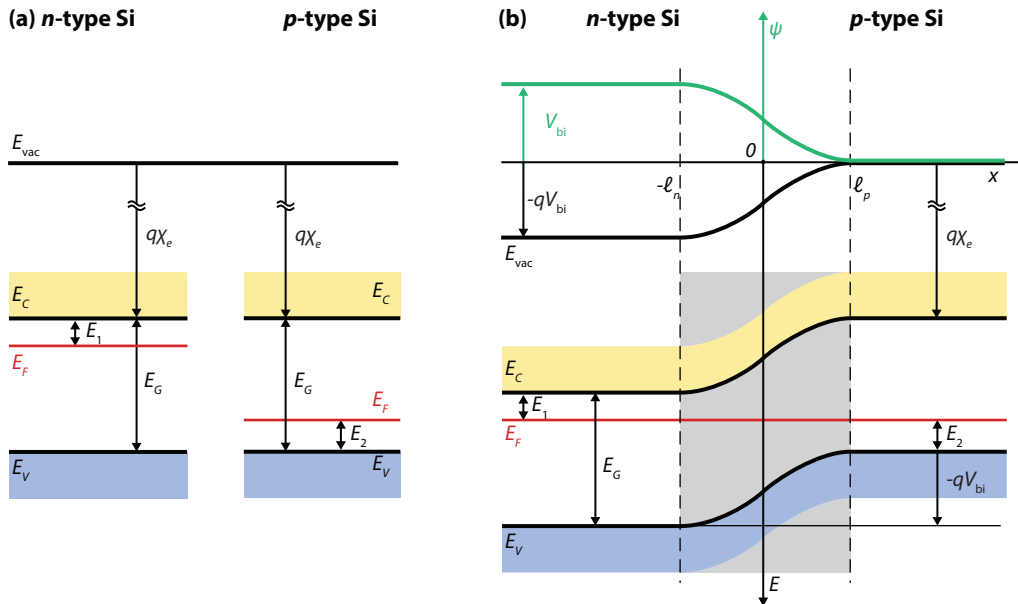
Figure 8.3: (a) The energy band diagrams of an *n*- and a *p*-type material that are separated from each other. (b) The energy-band diagram of the *p-n* junction under equilibrium. The electrostatic potential profile (green curve) is also presented in the figure.
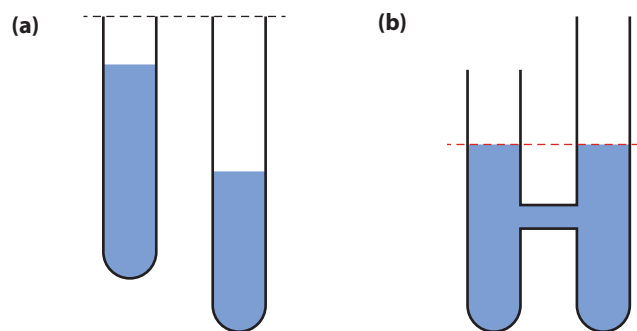
Figure 8.4: (a) Two tubes of different length (upper boundary represents vacuum level) and filling level (representing Fermi energy). (b) If the tubes are connected, the filling level will equalise but the heights of the tube boundaries can be different.
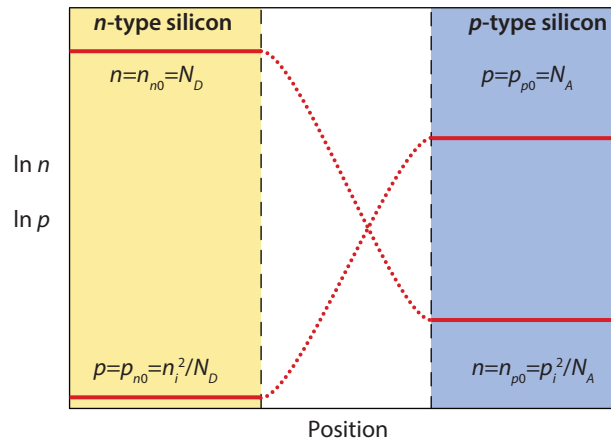
Figure 8.5: Concentrations profile of mobile charge carriers in a *p-n* junction under equilibrium.

energies E_C and E_V as well as the vacuum energy E_{vac} must be *continuous*. Hence, the bands get *bended*, which indicates the presence of an electric field in this region. Due to the electric field a difference in the electrostatic potential is created between the boundaries of the space-charge region. Across the depletion region the changes in the carrier concentration are compensated by changes in the electrostatic potential. The electrostatic-potential profile ψ is also drawn in Fig. 8.3 (b).

The concentration profile of charge carriers in a *p-n* junction is schematically presented in Fig. 8.5. In the quasi-neutral regions the concentration of electrons and holes is the same as in the isolated doped semiconductors. In the space-charge region the concentrations of majority charge carriers decrease very rapidly. This fact allows us to use the assumption that the space-charge region is depleted of mobile charge carriers. This assumption means that the charge of the mobile carriers represents a negligible contribution to the total space charge in the depletion region. The space charge in this region is fully determined by the ionised dopant atoms fixed in the lattice.

The presence of the internal electric field inside the *p-n* junction means that there is an electrostatic potential difference, V_{bi}, across the space-charge region. We shall determine a profile of the internal electric field and electrostatic potential in the *p-n* junction. First we introduce an approximation, which simplifies the calculation of the electric field and electrostatic-potential. This approximation (*the depletion approximation*) assumes that the space-charge density, ρ, is zero in the quasi-neutral regions and it is fully determined by the concentration of ionised dopants in the depletion region. In the depletion region of the *n*-type semiconductor it is the concentration of positively charged donor atoms, N_D, which determines the space charge in this region. In the *p*-type semiconductor, the concentration of negatively charged acceptor atoms, N_A, determines the space charge in the depletion region. This is illustrated in Fig. 8.6. Further, we assume that the *p-n* junction is a step junction; it means that there is an abrupt change in doping at the metallurgical junction and the doping concentration is uniform both in the *p*-type and the *n*-type semiconductors.

In Fig. 8.6, the position of the metallurgical junction is placed at zero, the width of
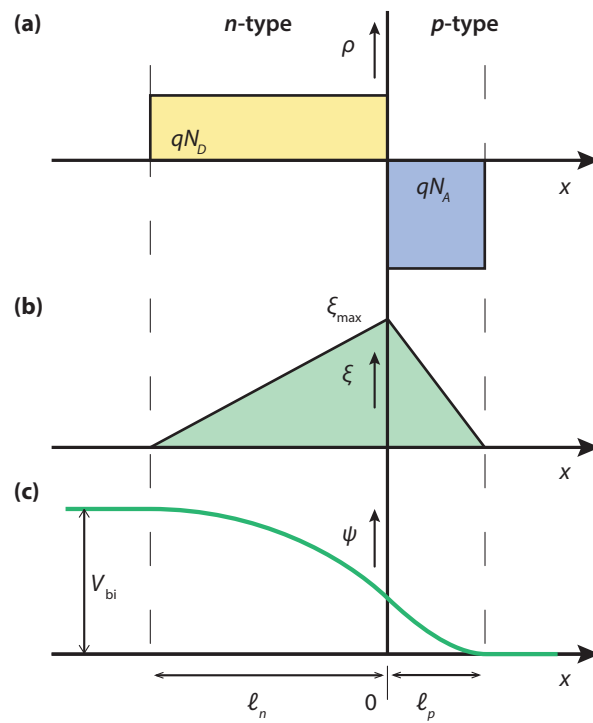
Figure 8.6: (a) The space-charge density $\rho(x)$, (b) the electric field $\xi(x)$, and (c) the electrostatic potential $\psi(x)$ across the depletion region of a *n-p* junction under equilibrium.

the space-charge region in the n-type material is denoted as ℓ_n and the width of the space-charge region in the p-type material is denoted as ℓ_p. The space-charge density is described by

$$\rho(x) = \quad qN_D \qquad \text{for} \qquad -\ell_n \leq x \leq 0, \tag{8.3a}$$
$$\rho(x) = -qN_A \qquad \text{for} \qquad 0 \leq x \leq \ell_p, \tag{8.3b}$$

where N_D and N_A is the concentration of donor and acceptor atoms, respectively. Outside the space-charge region the space-charge density is zero. The electric field which is calculated from the Poisson's equation, in one dimension can be written as

$$\frac{d^2\psi}{dx^2} = -\frac{d\xi}{dx} = -\frac{\rho}{\epsilon_r\epsilon_0}, \tag{8.4}$$

where ψ is the electrostatic potential, ξ is the electric field, ρ is the space-charge density, ϵ_r is the semiconductor dielectric constant and ϵ_0 is the vacuum permittivity. The vacuum permittivity is $= 8.854 \cdot 10^{-14}$ F/cm and for crystalline silicon $\epsilon_r = 11.7$. The electric field profile can be found by integrating the space-charge density across the space-charge region,

$$\xi = \frac{1}{\epsilon_r\epsilon_0}\int\rho\,dx. \tag{8.5}$$

Substituting the space-charge density with Eqs. (8.3) and using the boundary conditions

$$\xi(-\ell_n) = \xi(\ell_p) = 0, \tag{8.6}$$

we obtain as solution for the electric field

$$\xi(x) = \frac{q}{\epsilon_r\epsilon_0}N_D(\ell_n + x) \qquad \text{for} \qquad -\ell_n \leq x \leq 0, \tag{8.7a}$$
$$\xi(x) = \frac{q}{\epsilon_r\epsilon_0}N_A(\ell_p - x) \qquad \text{for} \qquad 0 \leq x \leq \ell_p. \tag{8.7b}$$

At the metallurgical junction, $x = 0$, the electric field is continuous, which requires that the following condition has to be fulfilled

$$N_A\ell_p = N_D\ell_n. \tag{8.8}$$

Outside the space-charge region the material is electrically neutral and therefore the electric field is zero there.

The profile of the electrostatic potential is calculated by integrating the electric field throughout the space-charge region and applying the boundary conditions,

$$\psi = -\int\xi\,dx. \tag{8.9}$$

We define the zero electrostatic potential level at the outside edge of the p-type semiconductor. Since we assume no potential drop across the quasi-neutral region the electrostatic potential at the boundary of the space-charge region in the p-type material is also zero,

$$\psi(\ell_p) = 0. \tag{8.10}$$

Using Eqs. (8.7) for describing the electric field in the n- and p-doped regions of the space-charge region, and taking into account that at the metallurgical junction the electrostatic potential is continuous, we can write the solution for the electrostatic potential as

$$\left.\begin{aligned} \psi\left(x\right) = &-\frac{q}{2\epsilon_r\epsilon_0}\, N_D\,\left(x+\ell_n\right)^2 \\ &+\frac{q}{2\epsilon_r\epsilon_0}\,\left(N_D\,\ell_n^2 + N_A\,\ell_p^2\right) \end{aligned}\right\} \qquad \text{for } -\ell_n \leq x \leq 0, \qquad (8.11a)$$

$$\psi\left(x\right) = \frac{q}{2\epsilon_r\epsilon_0}\, N_A\,\left(x-\ell_p\right)^2 \qquad \text{for } 0 \leq x \leq \ell_p. \qquad (8.11b)$$

Under equilibrium a difference in electrostatic potential, V_{bi}, develops across the space-charge region. The electrostatic potential difference across the p-n junction is an important characteristic of the junction and is denoted as the *built-in voltage* or diffusion potential of the p-n junction. We can calculate V_{bi} as the difference between the electrostatic potential at the edges of the space-charge region,

$$V_{bi} = \psi\left(-\ell_n\right) - \psi\left(\ell_p\right) = \psi\left(-\ell_n\right). \qquad (8.12)$$

Using Eq. (8.11a) we obtain for the built-in voltage

$$V_{bi} = \frac{q}{2\epsilon_r\epsilon_0}\,\left(N_D\,\ell_n^2 + N_A\,\ell_p^2\right) \qquad (8.13)$$

The built-in potential V_{bi} can also be determined with using the energy-band diagram presented in Fig. 8.3 (b).

$$qV_{bi} = E_G - E_1 - E_2. \qquad (8.14)$$

Using Eqs. (6.1) and (6.22), which determine the band gap, and the positions of the Fermi energy in the n- and p-type semiconductor, respectively,

$$E_G = E_C - E_V,$$
$$E_1 = E_C - E_F = k_B T\,\ln\left(N_C/N_D\right),$$
$$E_2 = E_F - E_V = k_B T\,\ln\left(N_V/N_A\right).$$

We can write

$$\begin{aligned} qV_{bi} &= E_G - k_B T\,\ln\left(\frac{N_V}{N_A}\right) - k_B T\,\ln\left(\frac{N_C}{N_D}\right) \\ &= E_G - k_B T\,\ln\left(\frac{N_V\,N_C}{N_A\,N_D}\right). \end{aligned} \qquad (8.15)$$

Using the relationship between the intrinsic concentration, n_i and the band gap, E_G [see Eq. (6.9)],

$$n_i^2 = N_C\,N_V\,\exp\left[-\frac{E_G}{k_B T}\right],$$

we can rewrite Eq. (8.15) and obtain

$$V_{bi} = \frac{k_B T}{q}\,\ln\left(\frac{N_A\,N_D}{n_i^2}\right) \qquad (8.16)$$

This equation allows us to determine the built-in potential of a *p-n* junction from the standard semiconductor parameters, such as doping concentrations and the intrinsic carrier concentration.

We can calculate the width of the space charge region of the *p-n* junction in the thermal equilibrium starting from Eq. (8.13). Using Eq. (8.8), either ℓ_n or ℓ_p can be eliminated from Eq. (8.13), resulting in expressions for ℓ_n and ℓ_p respectively,

$$\ell_n = \sqrt{\frac{2\epsilon_r\epsilon_0 V_{\text{bi}}}{q} \frac{N_A}{N_D} \left(\frac{1}{N_A + N_D} \right)}, \tag{8.17a}$$

$$\ell_p = \sqrt{\frac{2\epsilon_r\epsilon_0 V_{\text{bi}}}{q} \frac{N_D}{N_A} \left(\frac{1}{N_A + N_D} \right)}. \tag{8.17b}$$

The total space-charge width, W, is the sum of the partial space-charge widths in the *n*- and *p*-type semiconductors. Using Eq. (8.17) we find

$$W = \ell_n + \ell_p = \sqrt{\frac{2\epsilon_r\epsilon_0}{q} V_{\text{bi}} \left(\frac{1}{N_A} + \frac{1}{N_D} \right)}. \tag{8.18}$$

The space-charge region is not uniformly distributed in the *n*- and *p*- regions. The widths of the space-charge region in the *n*- and *p*-type semiconductor are determined by the doping concentrations as illustrated by Eqs. (8.17). Knowing the expressions for ℓ_n and ℓ_p we can determine the maximum value of the internal electric field, which is at the metallurgical junction. By substituting ℓ_p from expressed by Eq. (8.17b) into Eq. (8.7b) we obtain the expression for the maximum value of the internal electric field,

$$\xi_{\text{max}} = \sqrt{\frac{2q}{\epsilon_r\epsilon_0} V_{\text{bi}} \left(\frac{N_A N_D}{N_A + N_D} \right)}. \tag{8.19}$$

Example

A crystalline silicon wafer is doped with 10^{16} acceptor atoms per cubic centimetre. A 1 micrometer thick emitter layer is formed at the surface of the wafer with a uniform concentration of 10^{18} donors per cubic centimetre. Assume a step p-n junction and that all doping atoms are ionised. The intrinsic carrier concentration in silicon at 300 K is $1.5 \cdot 10^{10}$ cm^{-3}.

Let us calculate the electron and hole concentrations in the p- and n-type quasi-neutral regions at thermal equilibrium. We shall use Eqs. (8.1) and (8.2) to calculate the charge carrier concentrations.

P-type region: $p = p_{p0} \approx N_A = 10^{16}$ cm^{-3}.

$n = n_{p0} = n_i^2 / p_{p0} = \left(1.5 \cdot 10^{10} \right)^2 / 10^{16} = 2.25 \cdot 10^4$ cm^{-3}

N-type region: $n = n_{n0} \approx N_A = 10^{18}$ cm^{-3}.

$p = p_{n0} = n_i^2 / n_{n0} = \left(1.5 \cdot 10^{10} \right)^2 / 10^{18} = 2.25 \cdot 10^2$ cm^{-3}

We can calculate the position of the Fermi energy in the quasi-neutral n-type and p-type regions,

respectively, using Eq. (6.22a). We assume that the reference energy level is the bottom of the conduction band, $E_C = 0$ eV.

N-type region: $E_F - E_C = -k_B T \ln (N_C/n) = -0.0258 \ln \left(3.32 \cdot 10^{19} / 10^{18} \right) = -0.09$ eV.

P-type region: $E_F - E_C = -k_B T \ln (N_C/n) = -0.0258 \ln \left(3.32 \cdot 10^{19} / 2.24 \cdot 10^4 \right) = -0.90$ eV.

The minus sign tells us that the Fermi energy is positioned below the conduction band.
   The built-in voltage across the p-n junction is calculated using Eq. (8.16),

$$V_{bi} = \frac{k_B T}{q} \ln \left(\frac{N_A \, N_D}{n_i^2} \right) = 0.0258\,\text{V} \left[\frac{10^{16}\, 10^{18}}{(1.5 \cdot 10^{10})^2} \right] = 0.81\,\text{V}.$$

The width of the depletion region is calculated from Eq. (8.18),

$$W = \sqrt{ \frac{2 \epsilon_r \epsilon_0}{q} V_{bi} \left(\frac{1}{N_A} + \frac{1}{N_D} \right) } = \sqrt{ \frac{2 \cdot 11.7 \cdot 8.854 \cdot 10^{-14}}{1.602 \cdot 10^{-19}} \cdot 0.81 \left(\frac{1}{10^{16}} + \frac{1}{10^{18}} \right) }$$

$$= 3.25 \cdot 10^{-5}\,\text{cm} = 0.325\,\mu\text{m}.$$

A typical thickness of c-Si wafers is 300 μm. The depletion region is 0.3 μm which represents 0.1% of the wafer thickness. It is important to realise that almost the whole bulk of the wafer is a quasi-neutral region without an internal electrical field.
   *The maximum electric field is at the metallurgical junction and is calculated from Eq. (8.19).*

$$\zeta_{\text{max}} = \sqrt{ \frac{2q}{\epsilon_r \epsilon_0} V_{bi} \left(\frac{N_A \, N_D}{N_A + N_D} \right) } = \frac{2 \cdot 1.602 \cdot 10^{-19}}{11.7 \cdot 8.854 \cdot 10^{-14}} \cdot 0.81 \left(\frac{10^{16}\, 10^{18}}{10^{16} + 10^{18}} \right) = 5 \cdot 10^4\,\text{V cm}^{-1}.$$

8.1.3   The *p-n* junction under applied voltage

When an external voltage, V_a, is applied to a *p-n* junction the potential difference between the *n*- and *p*-type regions will change and the electrostatic potential across the space-charge region will become $(V_{\text{bi}} - V_a)$. Remember that under equilibrium the built-in potential is negative in the *p*-type region with respect to the *n*-type region. When the applied external voltage is negative with respect to the potential of the *p*-type region, the applied voltage will increase the potential difference across the *p-n* junction. We refer to this situation as *p-n* junction under *reverse-bias voltage*. The potential barrier across the junction is increased under reverse-bias voltage, which results in a wider space-charge region.

   Figure 8.7 (a) shows the band diagram of the *p-n* junction under reverse-biased voltage. Under external voltage the *p-n* junction is not under equilibrium any more and the concentrations of electrons and holes are described by the quasi-Fermi energy for electrons, E_{Fn}, and the quasi-Fermi energy for holes, E_{Fp}, respectively. When the applied external voltage is positive with respect to the potential of the *p*-type region, the applied voltage will decrease the potential difference across the *p-n* junction. We refer to this situation as *p-n* junction under *forward-bias voltage*. The band diagram of the *p-n* junction under forward-biased voltage is presented in Fig. 8.7 (b). The potential barrier across the junction is decreased under forward-bias voltage and the space charge region becomes narrower.
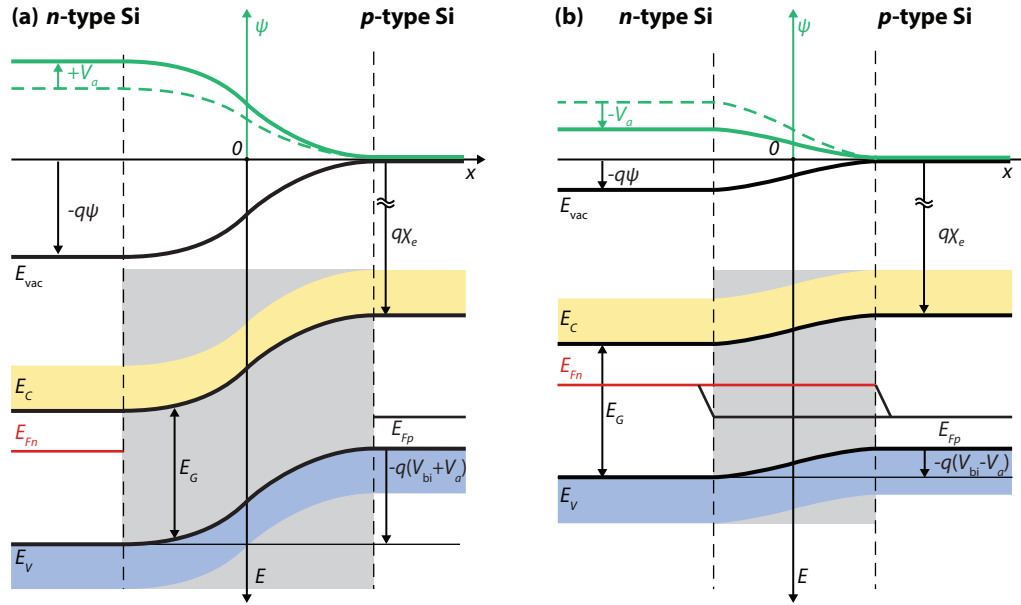
Figure 8.7: Energy band diagram and electrostatic-potential (in green) of a *p-n* junction under (a) reverse bias and (b) forward bias conditions.

The balance between the forces responsible for diffusion (concentration gradient) and drift (electric field) is disturbed. Lowering the electrostatic potential barrier leads to a higher concentration of minority carriers at the edges of the space-charge region compared to the situation in equilibrium. This process is referred to as minority-carrier *injection*. This gradient in concentration causes the diffusion of the minority carriers from the edge into the bulk of the quasi-neutral region.

The diffusion of minority carriers into the quasi-neutral region causes a so-called re-combination current density, J_{rec}, since the diffusing minority carriers recombine with the majority carriers in the bulk. The recombination current is compensated by the so-called thermal generation current, J_{gen}, which is caused by the drift of minority carriers, which are present in the corresponding doped regions (electrons in the *p*-type region and holes in the *n*-type region), across the junction. Both, the recombination and generation current densities have contributions from electrons and holes. When no voltage is applied to the *p-n* junction, the situation inside the junction can be viewed as the balance between the recombination and generation current densities,

$$J = J_{rec} - J_{gen} = 0 \qquad \text{for } V_a = 0 \text{ V.} \qquad (8.20)$$

It is assumed that when a moderate forward-bias voltage is applied to the junction the recombination current density increases with the Boltzmann factor $\exp(eV_a/k_BT)$,

$$J_{rec}(V_a) = J_{rec}(V_a = 0) \, \exp\left(\frac{qV_a}{k_BT}\right). \qquad (8.21)$$

This assumption is called the *Boltzmann approximation*.

The generation current density, on the other hand, is almost independent of the potential barrier across the junction and is determined by the availability of the thermally-generated minority carriers in the doped regions,

$$J_{\text{gen}}(V_a) \approx J_{\text{gen}}(V_a = 0). \tag{8.22}$$

The external net-current density can be expressed as

$$
\begin{aligned}
J(V_a) &= J_{\text{rec}}(V_a) - J_{\text{gen}}(V_a) \\
&= J_0 \left[\exp\left(\frac{qV_a}{k_B T} \right) - 1 \right],
\end{aligned}
\tag{8.23}
$$

where J_0 is the saturation current density of the p-n junction, given by

$$J_0 = J_{\text{gen}}(V_a = 0). \tag{8.24}$$

Equation (8.23) is known as the *Shockley equation* that describes the current-voltage behaviour of an ideal p-n diode. It is a fundamental equation for microelectronics device physics. The saturation current density is also known as *dark current density*; its detailed derivation for the p-n junction is carried out in Appendix B.1. The saturation-current density is given by

$$J_0 = q \, n_i^2 \left(\frac{D_N}{L_N N_A} + \frac{D_P}{L_P N_D} \right). \tag{8.25}$$

The saturation-current density depends in a complex way on the fundamental semiconductor parameters. Ideally the saturation-current density should be as low as possible and this requires an optimal and balanced design of the p-type and n-type semiconductor properties. For example, an increase in the doping concentration decreases the diffusion length of the minority carriers, which means that the optimal product of these two quantities requires a delicate balance between these two properties.

The recombination of the majority carriers due to the diffusion of the injected minority carriers into the bulk of the quasi-neutral regions results in a lowering of the concentration of the majority carriers compared to the one under equilibrium. The drop in the concentration of the majority carriers is balanced by the flow of the majority carriers from the electrodes into the bulk. In this way the net current flows through the p-n junction under forward-bias voltage. For high reverse-bias voltage, the Boltzmann factor in Eq. (8.23) becomes very small and can be neglected. The net current density is given by

$$J(V_a) = -J_0, \tag{8.26}$$

and represents the flux of thermally generated minority carriers across the junction. The current density-voltage (J-V) characteristic of an ideal p-n junction is schematically shown in Fig. 8.8.

8.1.4 The *p-n* junction under illumination

When a p-n junction is illuminated, additional electron-hole pairs are generated in the semiconductor. The concentration of minority carriers (electrons in the p-type region and holes in the n-type region) strongly increases, leading to the flow of the minority carriers
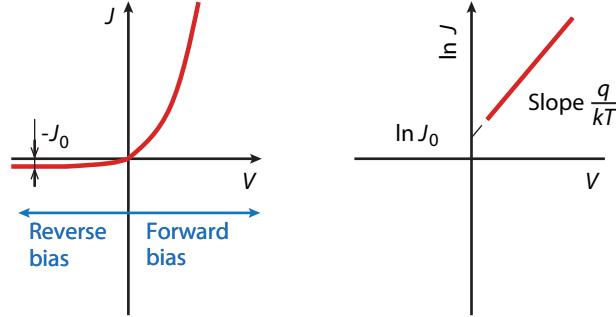
Figure 8.8: *J-V* characteristic of a *p-n* junction; (a) linear plot and (b) semi-logarithmic plot.

across the depletion region into the quasi-neutral regions. Electrons flow from the *p*-type into the *n*-type region and holes from the *n*-type into the *p*-type region. The flow of the photo-generated carriers causes the so-called *photo-generation current density*, J_{ph}, which adds to the thermal-generation current, J_{gen}. When no external electrical contact between the *n*-type and the *p*-type regions is established, the junction is in *open-circuit condition*. Hence, the current resulting from the flux of photo-generated and thermally-generated carriers has to be balanced by the opposite recombination current. The recombination current will increase through lowering of the electrostatic potential barrier across the depletion region.

The band diagram of the illuminated *p-n* junction under open-circuit condition is presented in Fig. 8.9 (a). As we have seen in Section 7.6, under non-equilibrium the Fermi level is replaced by quasi-Fermi levels that are different for electrons and holes and denote their electrochemical potential. Under open-circuit condition, the quasi-Fermi level of electrons, denoted by E_{Fn}, is higher than the quasi-Fermi level of holes (denoted by E_{Fp}) by an amount of qV_{oc}. This means that a voltmeter will measure a voltage difference of V_{oc} between the contacts of the *p-n* junction. We refer to V_{oc} as the *open-circuit voltage*.

The bands in the quasi-neutral regions (*i.e.* outside the depletion region) are flat. Under the assumption that the charge density in each of the regions is homogeneous, the bands follow a parabolic shape in the depletion region. In this case there is generation anywhere in the device. Under open circuit condition, the external current density is zero. So we have

$$J_n = J_{n,\,\text{drift}} + J_{n,\,\text{diff}} = q\mu_n nE + qD_n\frac{\mathrm{d}n}{\mathrm{d}x} = q\mu_n n\left(\frac{1}{q}\frac{\mathrm{d}E_C}{\mathrm{d}x}\right) + k_B T\mu_n\frac{\mathrm{d}n}{\mathrm{d}x}, \tag{8.27a}$$

$$J_p = J_{p,\,\text{drift}} + J_{p,\,\text{diff}} = q\mu_p pE - qD_n\frac{\mathrm{d}p}{\mathrm{d}x} = q\mu_p p\left(\frac{1}{q}\frac{\mathrm{d}E_V}{\mathrm{d}x}\right) - k_B T\mu_p\frac{\mathrm{d}p}{\mathrm{d}x}. \tag{8.27b}$$

The carrier densities are given by:

$$n = N_C \exp\left(-\frac{E_C - E_{Fn}}{k_B T}\right) \quad \text{and} \quad p = N_V \exp\left(-\frac{E_{Fp} - E_V}{k_B T}\right). \tag{8.28}$$
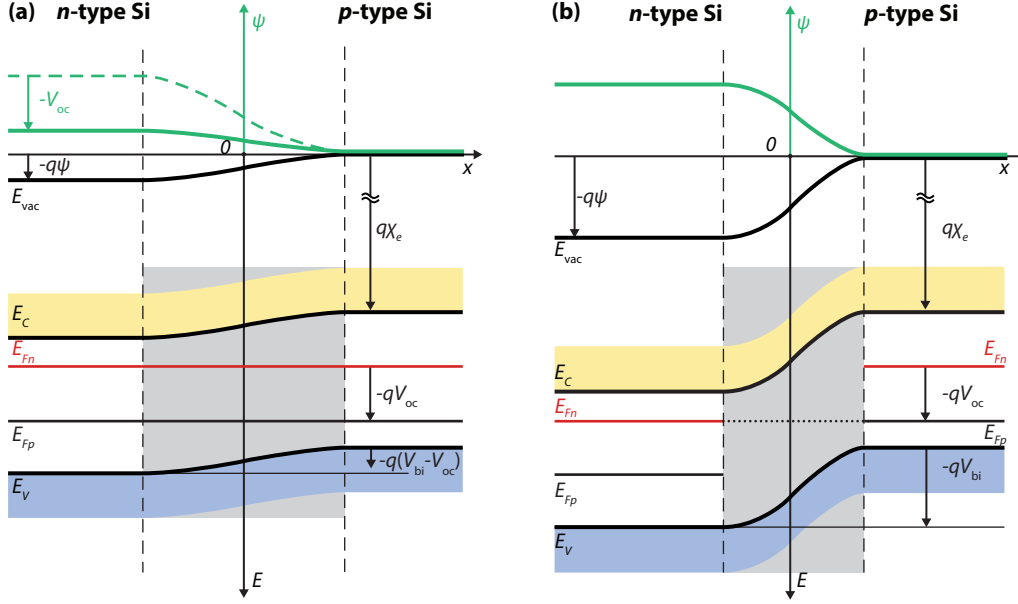
Figure 8.9: Energy band diagram and electrostatic-potential (in green) of an illuminated *p-n* junction under the (a) open-circuit and (b) short-circuit conditions.

So we find for the derivatives

$$\frac{dn}{dx} = -\frac{n}{k_B T}\left(\frac{dE_C}{dx} - \frac{dE_{Fn}}{dx}\right) \quad \text{and} \quad \frac{dp}{dx} = \frac{p}{k_B T}\left(\frac{dE_V}{dx} - \frac{dE_{Fp}}{dx}\right). \tag{8.29}$$

We then find for each current component

$$J_n = q\mu_n n\left(\frac{1}{q}\frac{dE_C}{dx}\right) + k_B T\mu_n\frac{dn}{dx} = \mu_n n\frac{dE_{Fn}}{dx}, \tag{8.30a}$$

$$J_p = q\mu_p p\left(\frac{1}{q}\frac{dE_V}{dx}\right) - k_B T\mu_p\frac{dp}{dx} = \mu_p n\frac{dE_{Fp}}{dx}. \tag{8.30b}$$

Hence, the total current is given by

$$J = J_n + J_p = \mu_n n\frac{dE_{Fn}}{dx} + \mu_p n\frac{dE_{Fp}}{dx} = 0. \tag{8.31}$$

Note that the last step implies that the current density at $V = V_{oc}$ is zero. The current density can only be zero if

$$\frac{dE_{Fn}}{dx} \equiv \frac{dE_{Fp}}{dx} \equiv 0, \tag{8.32}$$

which implies that the quasi-Fermi levels are horizontal in the entire band diagram of the solar cell.

Figure 8.9 (b) shows the band diagram of the *short-circuited p-n* junction. Under this situation, the photo-generated current will also flow through the external circuit. Under

the short-circuit condition the electrostatic-potential barrier is not changed, but from a strong variation of the quasi-Fermi levels inside the depletion region one can determine that the current is flowing inside the semiconductor.

When a load is connected between the electrodes of the illuminated *p-n* junction, only a fraction of the photo-generated current will flow through the external circuit. The electro-chemical potential difference between the *n*-type and *p*-type regions will be lowered by a voltage drop over the load. This in turn lowers the electrostatic potential over the depletion region which results in an increase of the recombination current. In the *superposition approximation*, the net current flowing through the load is determined as the sum of the photo- and thermal generation currents and the recombination current. The voltage drop at the load can be simulated by applying a forward-bias voltage to the junction, therefore Eq. (8.23), which describes the behaviour of the junction under applied voltage, is included to describe the net current of the illuminated *p-n* junction,

$$
\begin{aligned}
J\left(V_a\right) &= J_{\text{rec}}\left(V_a\right) - J_{\text{gen}}\left(V_a\right) - J_{\text{ph}} \\
&= J_0\left[\exp\left(\frac{qV_a}{k_BT}\right) - 1\right] - J_{\text{ph}}.
\end{aligned}
\tag{8.33}
$$

Both the dark and illuminated *J-V* characteristics of the *p-n* junction are represented in Fig. 8.10. Note that in the figure the superposition principle is reflected. The illuminated *J-V* characteristic of the *p-n* junction is the same as the dark *J-V* characteristic, but it is shifted down by the photo-generated current density J_{ph}. The detailed derivation of the photo-generated current density of the *p-n* junction is carried out in Appendix B.2. Under a uniform generation rate, G, its value is

$$
J_{\text{ph}} = qG\left(L_N + W + L_P\right),
\tag{8.34}
$$

where L_N and L_P are the minority-carrier-diffusion length for electrons and holes, respectively, and W is the width of the depletion region. It means that only carriers generated in the depletion region and in the regions up to the minority-carrier-diffusion length from the depletion region can contribute to the photo-generated current. When designing the thickness of a solar cell, Eq. (8.34) must be considered. The thickness of the absorber should not be thicker than the region from which the carriers contribute to the photo-generated current.

8.2 Heterojunctions

In the previous sections we discussed the physics of junctions between an *n*-doped and a *p*-doped semiconductor of the same material. In these junctions, that are called *homojunctions*, the bandgap and the electron affinity are the same at both sides of the junction. Of course, junctions between different materials can also be made. These junctions are called *heterojunctions*. Heterojunctions are very important for solar cells; in fact, as of 2014, the best solar cells based on crystalline silicon have heterojunctions of crystalline and amorphous silicon, as we will see in Chapter 12. In this section we will look at the most important features of heterojunctions.

We can distinguish between four types of heterojunctions: *n-P* junctions, *p-N* junctions, *n-N* junctions, and *p-P* heterojunctions, where the lower-case letter denotes the material